Analysis of Power and Power Spectral Density for Quaternary Random Pulse Position Modulation

Hung-Chi Chen
Department of Electronics and Electrical Engineering
National Yang Ming Chiao Tung University (NYCU)
Hsinchu, Taiwan, (R.O.C.)
hcchen @nycu.edu.tw

Hsiang-Kai, Wu
Institute of Electrical and Control Engineering
National Yang Ming Chiao Tung University (NYCU)
Hsinchu, Taiwan (R.O.C.)
hcchen @nycu.edu.tw

Chih-Chiang Wu
Mechanical and Mechatronics Systems Research Laboratories,
Industrial Technology Research Institute (ITRI),
Hsinchu, Taiwan (R.O.C.)
John.Wu@itri.org.tw

***Abstract*—In this paper, the quaternary random pulse position modulation (QRPPM) is proposed to further reduce the power of dominant harmonic clusters. From the analysis of the power and power spectral density, the minimum integer-harmonics power dispersion rate (HPDR) is increased from 50.0% of the conventional random center/edge alignment PWM (RCEA-PWM) to 75.0% of the proposed QRPPM. Some results are provided to validate the proposed method.**

Keywords—harmonic spread, power spectral density, random pulse position modulation

I. INTRODUCTION

The conventional PWM strategy is widely used in DC-DC converters due to its simplicity. However, this strategy generates the deterministic switching signals and contributes to the concentration of harmonic energy at the specific frequency. The dominant harmonic clusters may lead to increased EMI [1-3].

Some random pulse position modulation (RPPM) techniques had been developed to disperse some integer-harmonic energy. Fig. 1. shows two common RPPMs.

In Fig. 1(a), two deterministic signals with the same duty ratio are generated from the comparisons of the control signal and two saw-teeth signals [4]. Since one of two deterministic signals always begins with "High" and the other always begins with "Low" within every time slots, it is also named random lead-lag (RLL) PWM.

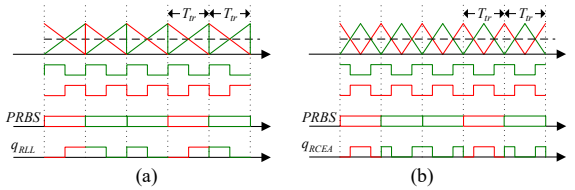

Fig. 1 Two common random pulse position modulations
(a) random lead-lag PWM (RLL-PWM) [4-5]
(b) random center/edge aligned PWM (RCEA-PWM)[6-9].

In Fig. 1(b), two deterministic signals with the same duty ratio are generated from the comparisons of one control signal and two triangular signals [5-8]. Since one of two deterministic signals always begins and ends with "High" and the other always begins and ends with "Low" within every time slots, it is also named random center/edge-aligned PWM (RCEA).

It is noted that RCEA-PWM possesses better integer-harmonics power dispersion performance than RLL-PWM. Thus, RCEA-PWM often cooperates with other random schemes to enhance the power dispersion performance.

In [7], random carrier frequency modulation (RCFM) was cooperated with RCEA-PWM. In [8], random pulse number modulation (RPNM) was combined with RCEA-PWM. Table I tabulates the comparison of various RPPM. The integer-harmonics power dispersion rate is defined to evaluate the power dispersion performance. For the conventional PWM, PWM's power is concentrated at the integer multiplies of the switching frequency. Thus, PWM's HPDR is 0% in Table I.

Due to randomness, some concentrated power may be dispersed, and thus HPDR of random modulation may be larger than 0%. It is noted that power dispersion rate is dependent on the duty ratio, and RLL and RCEA yield the peak HPDR 100% at the duty ratio 0.5.

Table I. Summary of various RPPM

	PWM	RLL	RCEA	QRPPM
Triangular Frequency	f_{tr}	f_{tr}	f_{tr}	f_{tr}
Average Switching Frequency	f_{tr}	$0.75f_{tr}$	$1.25f_{tr}$	$1.1875f_{tr}$
1st nonzero harmonic Frequency	f_{tr}	f_{tr}	$2f_{tr}$	$4f_{tr}$
HPDR	0%	50%~100%	50%~100%	75%~100%

Since the switching signals of the random modulation are not deterministic, the power spectrum may include the continuous and discrete parts [10-12].

Normally, the popular Fourier transform (FT) can be used to obtain the deterministic signal's spectral characteristics and its frequency domain distribution. However, the FT may not clearly describe the frequency domain characteristics of non-deterministic signals.

For random signals, analyzing their spectrum with the FT is possible, but the result is not comprehensive since the amplitude at each frequency represents just one sample within the signal's sample space.

Thus, power spectral density (PSD) are widely used to evaluate the spectral distribution of a random signal [6, 13]. However, PSD can also be used to evaluate the spectral harmonics of a deterministic signal.

In this paper, the quaternary random pulse position modulation (QRPPM) is proposed and its integer-harmonics power dispersion effect is evaluated by the analysis of power and power spectral density. The minimum power dispersion rate (PDR) is increased from 50% of the conventional random center/edge alignment PWM (RCEA-PWM) to 75.0% of the proposed QRPPM without the decrease of the switching number and switching loss. Some simulation and experimental results are provided to demonstrate the proposed QRPPM.

II. THE PROPOSED QRPPMS

The block diagram of the proposed QRPPM is plotted in Fig. 2(a) where the random signal *PRBS* changes within every fixed time period T_{tr} and selects one of four pulse signals to generate the proposed pulse signal $q_{QRPPM}(t)$.

Four deterministic pulse signals $q_1(t)$, $q_2(t)$, $q_3(t)$ and $q_4(t)$ are generated from the comparisons of the control signal $v_{cont}(t)$ and four interleaved triangular signals $v_{tr1}(t)$, $v_{tr2}(t)$, $v_{tr3}(t)$ and $v_{tr4}(t)$ with the unified amplitude $\hat{v}_{tr}$. Thus, all four pulse signals yield the same duty ratio d. The duty ratio d of the pulse signals can be expressed by

$$d = \frac{v_{cont}}{\hat{v}_{tr} = \hat{v}_{tr1} = \hat{v}_{tr2} = \hat{v}_{tr3} = \hat{v}_{tr4}} \tag{1}$$

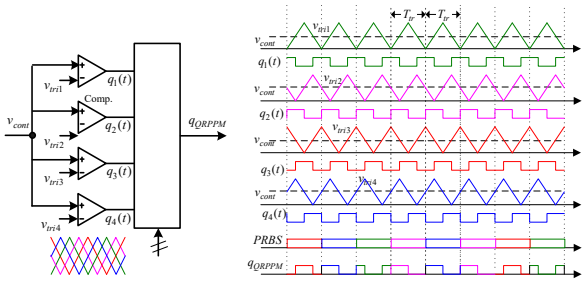

(a) (b)

Fig. 2 (a) Block diagram of the proposed QRPPM;
(b) illustrated waveforms of the proposed QRPPM.

From the illustrated waveforms in Fig. 2(b), four pulse signals during $nT_{tr} \le t \le (n+1)T_{tr}$ can be expressed by

$$\begin{aligned} q_1(t) = {} & u(t-nT_{tr}) - u\left(t-nT_{tr}-\frac{dT_{tr}}{2}\right) \\ & + u\left(t-(n+1)T_{tr}+\frac{dT_{tr}}{2}\right) - u\left(t-(n+1)T_{tr}\right) \end{aligned} \tag{2}$$

$$q_2(t) = \begin{cases} u\left(t-nT_{tr}-(\frac{T_{tr}}{4}-\frac{dT_{tr}}{2})\right) \\ \quad -u\left(t-nT_{tr}-(\frac{T_{tr}}{4}+\frac{dT_{tr}}{2})\right), & \text{when } 0 \le d \le \frac{1}{2} \\ u\left(t-nT_{tr}\right)-u\left(\begin{matrix}t-nT_{tr} \\ -(\frac{T_{tr}}{4}+\frac{dT_{tr}}{2})\end{matrix}\right) \\ \quad +u\left(\begin{matrix}t-(n+1)T_{tr} \\ -(\frac{T_{tr}}{4}-\frac{dT_{tr}}{2})\end{matrix}\right)-u\left(t-(n+1)T_{tr}\right), & \text{when } \frac{1}{2} \le d \le 1 \end{cases} \tag{3}$$

$$q_3(t) = u\left(t-nT_{tr}-(\frac{T_{tr}}{2}-\frac{dT_{tr}}{2})\right) - u\left(t-nT_{tr}-(\frac{T_{tr}}{2}+\frac{dT_{tr}}{2})\right) \tag{4}$$

$$q_4(t) = \begin{cases} u\left(t-nT_{tr}-(\frac{3T_{tr}}{4}-\frac{dT_{tr}}{2})\right) \\ \quad -u\left(t-nT_{tr}-(\frac{3T_{tr}}{4}+\frac{dT_{tr}}{2})\right), & \text{when } 0 \le d \le \frac{1}{2} \\ u\left(t-nT_{tr}\right)-u\left(\begin{matrix}t-nT_{tr} \\ +(\frac{T_{tr}}{4}-\frac{dT_{tr}}{2})\end{matrix}\right) \\ \quad +u\left(\begin{matrix}t-nT_{tr} \\ -(\frac{3T_{tr}}{4}-\frac{dT_{tr}}{2})\end{matrix}\right)-u\left(t-(n+1)T_{tr}\right), & \text{when } \frac{1}{2} \le d \le 1 \end{cases} \tag{5}$$

The random signal PRBS may be 00, 01, 10 and 11 with equal possibility 1/4. The pulse signal $q_{QRPPM}(t)$ can be expressed by

$$q_{QRPPM}(t) = \begin{cases} q_1, \textit{ when } \text{PRBS} = 00 \\ q_2, \textit{ when } \text{PRBS} = 01 \\ q_3, \textit{ when } \text{PRBS} = 10 \\ q_4, \textit{ when } \text{PRBS} = 11 \end{cases} \tag{6}$$

To calculate the average switching number per second, the illustrated classifications with duty ratio <0.5 are plotted in Fig. 3. From Fig. 3(a), when the PRBS is 01, 10 and 11, the selected pulses begin and end with "Low", and thus, the switching number is counted by 1.

From Fig. 3(b), when the PRBS is 00, the pulse signal $q_1(t)$ is selected and it begins with "High", goes to "Low", returns to "High" and ends with "High", and the switching number may be counted by more than 1.

If the previous pulse ends with "Low", the switching number should be additionally counted by 0.5. If the next pulse begins with "Low", the switching number should be additionally counted by 0.5.

With considering the possibility, the average switching number is calculated by 1+1/4*3/4*1/2+1/4*3/4*1/2=19/16.

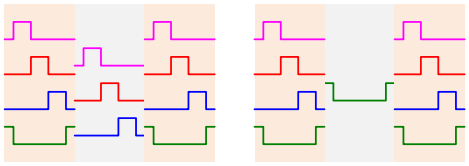

(a) (b)

Fig. 3 Classifications of the proposed pulse signal with duty ratio d<0.5
(a) the cases of the switching number counted by 1;
(b) the case of the switching number counted by more than 1.

The illustrated classifications with duty ratio >0.5 are plotted in Fig. 4. From Fig. 4(a), when the PRBS is 10, the selected pulse begins and ends with "Low", and thus, the switching number is counted by 1.

From Fig. 4(b), the selected pulses begin with "High", go to "Low", return to "High" and end with "High", and the switching number may be counted by more than 1.

If the previous pulse ends with "Low", the switching number should be additionally counted by 0.5. If the next pulse begins with "Low", the switching number should be additionally counted by 0.5.

With considering the possibility, the average switching number is calculated by 1+3/4*1/4*1/2+3/4*1/4*1/2=19/16.

It follows that the proposed QRPPM yields the average switching frequency $1.1875 f_{tr}$.

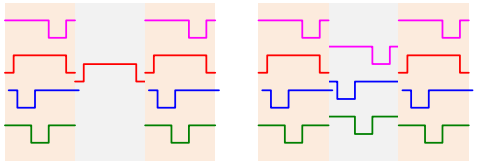

(a) (b)

Fig. 4 Classifications of the proposed pulse signal with duty ratio d>0.5
(a) the cases of the switching number counted by 1;
(b) the case of the switching number counted by more than 1.

III. Power Spectral Density Anaysis

In dc/dc converter, the output voltage is dependent on the switching signal. Thus, the analysis of power spectral density of the pulse signal $q_{QRPPM}(t)$ is able to evaluate the power distribution of the proposed strategie.

The power spectral density PSD $S_q(f)$ of the combined pulse signal $q_{QRPPM}(t)$ consists of the dc PSD component $S_q^{dc}(f=0)$, the integer-harmonics PSD $S_q^h(f=nf_{tr})$ and the other continuous PSD component $S_q^c(f)$.

$$S_q(f)=S_q^{dc}(f=0)+S_q^h(f=nf_{tr})+S_q^c(f) \tag{7}$$

$$S_q^{dc}(0)=\frac{\int_0^{T_{tr}} q(t)dt}{T_{tr}}\delta(0) \tag{8}$$

$$S_q^h(f=nf_{tr})=\sum_{n=1}^{\infty}\left(2\left|E\left[Q(nf_{tr})\right]\right|^2(f_{tr})^2\delta(f-nf_{tr})\right) \tag{9}$$

$$S_q^c(f)=(f_{tr})\left(E\left[\left|Q(f)\right|^2\right]-\left|E\left[Q(f)\right]\right|^2\right) \tag{10}$$

where $f_{tr}=1/T_{tr}$ is the triangle frequency, and $E[.]$ represents the operator for taking the expected value across the entire FT ensemble of the possible deterministic pulse signals. For a pulse signal $q_{QRPPM}(t)$ with fixed duty ratio d within every period T_{tr}, the dc PSD component is $S_q^{dc}(f=0)=d\cdot\delta(0)$ and thus, the dc power is d^2.

The integer-harmonics power P_q^h can be calculated from the integer-harmonics PSD $S_q^h(f)$.

$$P_q^h=\sum_{\text{int}\,n=1}^{\infty}\left(2\left|E\left[Q(nf_{tr})\right]\right|^2(f_{tr})^2\right) \tag{11}$$

Similarly, the power P_q^c can be obtained from the continuous PSD component.

$$P_q^c=2\int_{0^+}^{\infty}S_q^c(f)df=P_q-P_q^{dc}-P_q^h \tag{12}$$

where P_q is the total power of the pulse signal $q_{QRPPM}(t)$, and it is equal to the sum $P_q=P_q^{dc}+P_q^h+P_q^c$.

For any comparison signal $q_{QRPPM}(t)$ varying between 0 and 1 with the fixed duty ratio d within each triangle period T_{tr}, the rms value of $q_{QRPPM}(t)$ is $q_{rms}=\sqrt{d}$, and thus, the total power of the signal $q_{QRPPM}(t)$ is $P_q=(\sqrt{d})^2=d$. Because that the dc value of the signal $q_{QRPPM}(t)$ is d, and thus, the dc power P_q^{dc} of the signal $q_{QRPPM}(t)$ is $P_q^{dc}=d^2$. From (12), the sum of the integer-harmonics power P_q^h and the power P_q^c is constant $P_q^c+P_q^h=d-d^2$ [13].

If the pulse signal is deterministic, the continuous PSD component $S_q^c(f)$ must be zero, and thus, the power P_q^c is zero. It follows that the integer-harmonics power P_q^h is $P_q^h=P_q-P_q^{dc}=d-d^2$ for a deterministic signal and there is no integer-harmonics power dispersion.

For a nondeterministic comparison signal with fixed duty ratio d, the continuous PSD component $S_q^c(f)$ must be larger than zero, and the power P_q^c must be larger than zero. That is, the integer-harmonics power is $P_q^h=P_q-P_q^{dc}-P_q^c<P_q-P_q^{dc}=d-d^2$.

That is, the strategy generating the nondeterministic comparison signal may disperse some integer-harmonics power P_q^h to the power P_q^c due to the constant $P_q^c+P_q^h=d-d^2$. The power dispersion effect is evaluated by the defined integer-harmonics power dispersion ratio ξ (HPDR).

$$\xi=\frac{P_q^c}{P_q^h+P_q^c}=\frac{P_q^c}{d-d^2}*100\% \tag{13}$$

The Fourier transform (FT) $Q_1(f)$, $Q_2(f)$, $Q_3(f)$ and $Q_4(f)$ of the deterministic pulse signals can be expressed by

$$Q_1(f)=\frac{\sin(\pi fdT_{tr})}{\pi f}\left[\cos(2\pi fT_{tr})-j\sin(2\pi fT_{tr})\right] \tag{14}$$

$$Q_2(f)=\int_{\frac{T_{tr}}{4}-\frac{dT_{tr}}{2}}^{\frac{T_{tr}}{4}+\frac{dT_{tr}}{2}}e^{-j2\pi ft}dt=\int_{\frac{T_{tr}}{4}-\frac{dT_{tr}}{2}}^{\frac{T_{tr}}{4}+\frac{dT_{tr}}{2}}\frac{de^{-j2\pi ft}}{(-j2\pi f)}=\frac{\sin(\pi fdT_{tr})}{\pi f}\begin{bmatrix}\cos\left(\frac{\pi fT_{tr}}{2}\right)\\ -j\sin\left(\frac{\pi fT_{tr}}{2}\right)\end{bmatrix} \tag{15}$$

$$Q_3(f)=\frac{\sin(\pi fdT_{tr})}{\pi f}\left[\cos(\pi fT_{tr})-j\sin(\pi fT_{tr})\right] \tag{16}$$

$$Q_4(f)=\int_{\frac{3T_{tr}}{4}-\frac{dT_{tr}}{2}}^{\frac{3T_{tr}}{4}+\frac{dT_{tr}}{2}}e^{-j2\pi ft}dt=\int_{\frac{3T_{tr}}{4}-\frac{dT_{tr}}{2}}^{\frac{3T_{tr}}{4}+\frac{dT_{tr}}{2}}\frac{de^{-j2\pi ft}}{(-j2\pi f)}=\frac{\sin(\pi fdT_{tr})}{\pi f}\begin{bmatrix}\cos\left(\frac{3\pi fT_{tr}}{2}\right)\\ -j\sin\left(\frac{3\pi fT_{tr}}{2}\right)\end{bmatrix} \tag{17}$$

The expected value of the square amplitude of FT can be expressed by

$$E\left[\left|Q(f)\right|^2\right]=\frac{1}{4}\left|Q_1(f)\right|^2+\frac{1}{4}\left|Q_2(f)\right|^2+\frac{1}{4}\left|Q_3(f)\right|^2+\frac{1}{4}\left|Q_4(f)\right|^2 \tag{18}$$

The square $\left|E\left[Q(f)\right]\right|^2$ of the expected FT $E[Q(f)]$ can be expressed by

$$\left|E\left[Q(f)\right]\right|^2=\left|\frac{1}{4}Q_1(f)+\frac{1}{4}Q_2(f)+\frac{1}{4}Q_3(f)+\frac{1}{4}Q_4(f)\right|^2 \tag{19}$$

From (9), the integer-harmonics PSD component $S_{TRPPM}^h(f)$ can be derived by

$$S_{QRPPM}^h(f)=\sum_{n=1}^{\infty}\left(\frac{2\sin^2(dn4\pi)}{(4n\pi)^2}\delta(f-4nf_{tr})\right) \tag{20}$$

From (20), the integer-harmonics power P_{QRPPM}^h can be simplified to

$$P_{QRPPM}^h(d)=\begin{cases}-(d-\frac{1}{8})^2+\frac{1}{64}, & \text{when } 0\le d\le\frac{1}{4}\\ -(d-\frac{3}{8})^2+\frac{1}{64}, & \text{when } \frac{1}{4}\le d\le\frac{2}{4}\\ -(d-\frac{5}{8})^2+\frac{1}{64}, & \text{when } \frac{2}{4}\le d\le\frac{3}{4}\\ -(d-\frac{7}{8})^2+\frac{1}{64}, & \text{when } \frac{3}{4}\le d\le 1\end{cases} \tag{21}$$

The dispersion power P_{QRPPM}^c is equal to $P_{QRPPM}^c=d-d^2-P_{QRPPM}^h$.

For reference, the integer-harmonics power for RCEA-PWM is included here.

$$P_{RCEA}^h(d)=\sum_{n=1}^{\infty}\frac{\left[1+(-1)^n\right]\sin^2(dn\pi)}{(n\pi)^2}=\begin{cases}-(d-\frac{1}{4})^2+\frac{1}{16}, & \text{when } 0\le d\le 0.5\\ -(d-\frac{3}{4})^2+\frac{1}{16}, & \text{when } 0.5\le d\le 1.0\end{cases} \tag{22}$$

The derived power distribution are plotted in Fig. 5(a) and Fig. 5(b) where the **blue line** indicates the function $d-d^2=P^h_{QRPPM}+P^c_{QRPPM}$, the **gray line** indicates the integer-harmonic power P^h_{QRPPM} and the orange line is the dispersion power P^c_{QRPPM}. The proposed QRPPM yields larger dispersion power than the conventional RCEA-PWM. Fig. 3 plots the power dispersion ratio curves of the proposed QRPPM (**red line**) and the conventional RCEA-PWM (**black line**). Obviously, the minimum power dispersion ratio PDR is increased from 50% to 75%.

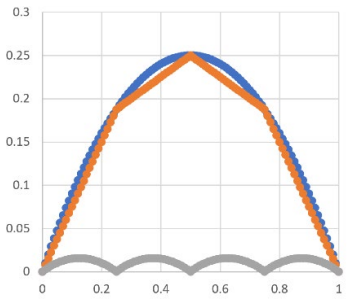

(a)

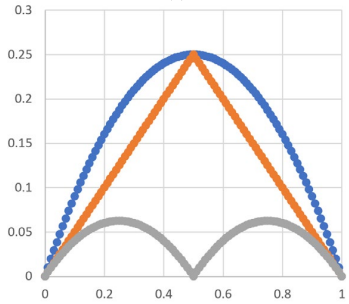

(b)

Fig. 5 Power distribution (a) the proposed QRPPM; (b) the conventional RCEA-PWM;

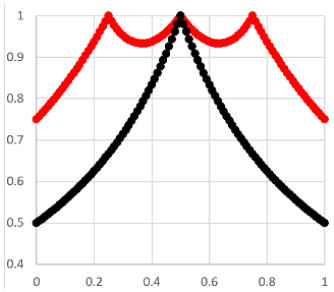

Fig. 6 HPDR of the proposed QRPPM (red line) and RCEA-PWM (black line).

IV. Simulation Results

To demonstrate the proposed QRPPM, the buck converter in Fig. 7 is setup, and its circuit parameters are tabulated in Table II.

The simulation results of the duty ratio d=1/4 with the conventional PWM, RCEA-PWM and the proposed QRPPM are plotted in Fig. 8 where Fig. 8(a) plots their switching signals and Fig. 8(b) plots FFT of the switching signals in Fig. 8(a).

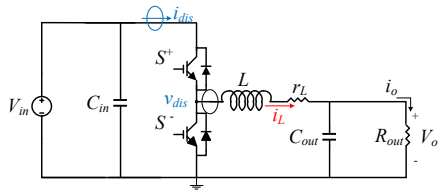

Fig. 7 Buck converter for demonstration.

TABLE II Circuit Parameters

PWM Schemes	Conventional PWM	RCEA-PWM	Proposed QRPPM
Triamgular Frequency f_{tr}	40kHz	40kHz	40kHz
Input Voltage V_{in}	200V		
Inductor L	2.24mH		
Output Capacitance C_{out}	300μF		
Load R_{out}	25Ω		

From Fig. 6 and (13), the curve at duty ratio d=0.25 shows that the HPDR of the proposed QRPPM is 100% and the HPDR of the RCEA-PWM is 66.7%.

It is obvious that from Fig. 8(b), some integer-harmonic power is dispersed by RCEA-PWM and all integer-harmonic power are dispersed by the proposed QRPPM.

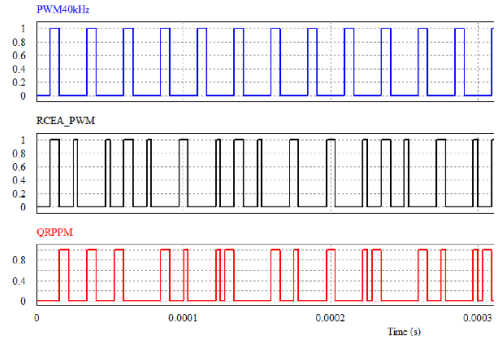

(a)

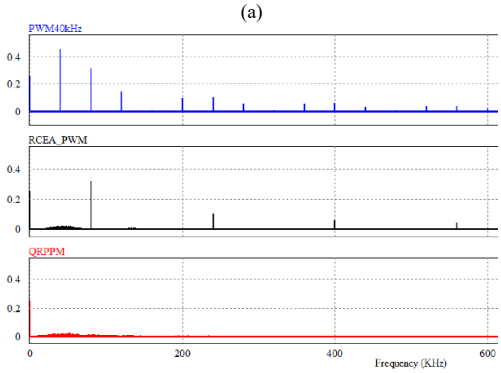

(b)

Fig. 8 Simulation results (d=1/4) of various PWM strategies: (a) switching signals; (b) FFT.

The simulation results of the duty ratio d=3/8 with PWM, RCEA-PWM and the proposed QRPPM are plotted in Fig. 9. In Fig. 6, the curve at duty ratio d=0.375 indicates that the HPDR of the proposed QRPPM is 93.3% and the HPDR of the RCEA-PWM is 80%. From Fig. 9(b), it is obvious that the proposed QRPPM disperses more integer-harmonic power than RCEA-PWM, and the first dominant integer-harmonic is located at 160kHz (i.e. $4f_{tr}$).

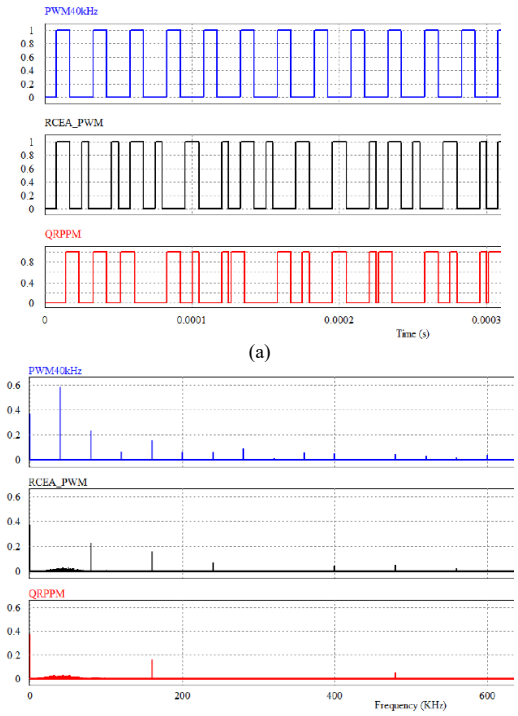

Fig. 9 Simulation results (d=3/8) of various PWM strategies: (a) switching signals; (b) FFT.

V. Experimental Results

Fig. 10 shows the implementation hardware in this paper, featuring a bidirectional DC-DC converter. The control circuit, developed on a Xilinx Spartan-6 series XC6SLX9 FPGA board, includes the controller, PWM strategy designs, and Analog-to-Digital conversion circuits.

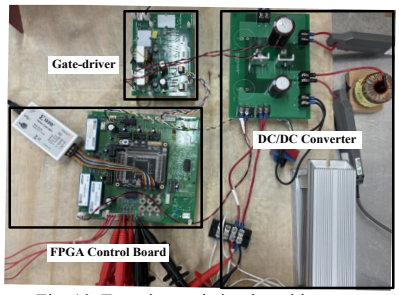

Fig. 10. Experimental circuit architecture.

Fig. 11 plots the FFTs of the switching voltage v_{dis} in buck converter by the proposed QRPPM where the digital oscilloscope R/S is used.

The proposed QRPPM shows superior power dispersion performance than the conventional PWM and RCEA especially at duty ratio d=0.25. From Fig. 11(b), the first dominant peak of QRPPM is located at 160kHz (i.e. $4f_{tr}$) larger than those of PWM and RCEA-PWM.

VI. Conclusion

In this paper, the proposed QRPPM shows superior power dispersion performance among the other RPPMs. In addition, the DC/DC converter would also benefit from the QRPPM's first dominant peak located at four time the triangular frequency.

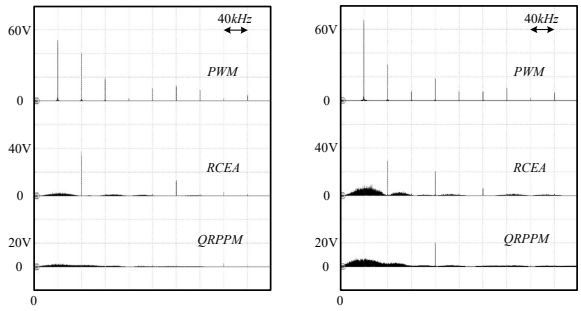

Fig. 11 FFT of the switching voltage v_{dis} in buck converter (a) d=1/4; (b) d=3/8.

References

[1] A. Vedde, M. Neuburger and H. Reuss, "An optimized high-frequency EMI filter design for an automotive DC/DC-converter," 2021 National Power Electronics Conference (NPEC), Bhubaneswar, India, 2021, pp. 01-06, doi: 10.1109/NPEC52100.2021.9672512.

[2] F. Mihali and D. Kos, "Reduced Conductive EMI in Switched-Mode DC–DC Power Converters Without EMI Filters: PWM Versus Randomized PWM," in *IEEE Transactions on Power Electronics*, vol. 21, no. 6, pp. 1783-1794, Nov. 2006, doi: 10.1109/TPEL.2006.882910.

[3] S. Kaboli, J. Mahdavi, and A. Agah, "Application of random PWM technique for reducing the conducted electromagnetic emissions in active filters," in *IEEE Transactions on Industrial Electronics*, vol. 54, no. 4, pp. 2333–2343, Aug. 2007.

[4] Y. -C. Lim, S. -O. Wi, J. -N. Kim and Y. -G. Jung, "A Pseudorandom Carrier Modulation Scheme," in *IEEE Transactions on Power Electronics*, vol. 25, no. 4, pp. 797-805, April 2010, doi: 10.1109/TPEL.2009.2035699.

[5] M. M. Bech, F. Blaabjerg and J. K. Pedersen, "Random modulation techniques with fixed switching frequency for three-phase power converters," in *IEEE Transactions on Power Electronics*, vol. 15, no. 4, pp. 753-761, July 2000, doi: 10.1109/63.849046.

[6] Bor-Ren Lin, "Implementation of nondeterministic pulse width modulation for inverter drives," in *IEEE Transactions on Aerospace and Electronic Systems*, vol. 36, no. 2, pp. 482-490, April 2000, doi: 10.1109/7.845228.

[7] H. C. Chen, Y. F. Tsai and W. C. Tsai, "Analysis of Random Center/Edge Alignment PWM and its Application to Digital Current Control for Boost DC-DC Converters," 16th IEEE Energy Conversion Congress and Exposition (ECCE), Pheonix, USA, 2024.

[8] K. -S. Kim, Y. -G. Jung and Y. -C. Lim, "A New Hybrid Random PWM Scheme," in *IEEE Transactions on Power Electronics*, vol. 24, no. 1, pp. 192-200, Jan. 2009, doi: 10.1109/TPEL.2008.2006613.

[9] Y. -S. Lai, Y. -T. Chang and B. -Y. Chen, "Novel Random-Switching PWM Technique With Constant Sampling Frequency and Constant Inductor Average Current for Digitally Controlled Converter," in *IEEE Transactions on Industrial Electronics*, vol. 60, no. 8, pp. 3126-3135, Aug. 2013, doi: 10.1109/TIE.2012.2201436.

[10] A. M. Stankovic, G. E. Verghese and D. J. Perreault, "Analysis and synthesis of randomized modulation schemes for power converters," in *IEEE Transactions on Power Electronics*, vol. 10, no. 6, pp. 680-693, Nov. 1995, doi: 10.1109/63.471288.

[11] K. K. Tse, H. S. -H. Chung, S. Y. R. Hui and H. C. So, "A comparative investigation on the use of random modulation schemes for DC/DC converters," in *IEEE Transactions on Industrial Electronics*, vol. 47, no. 2, pp. 253-263, April 2000, doi: 10.1109/41.836340.

[12] Y. Shrivastava, S. Sathiakumar and V. G. Agelidis, "Analysis and Verification of Two-Level Random Aperiodic PWM Schemes for DC–DC Converters," in *IEEE Transactions on Power Electronics*, vol. 24, no. 9, pp. 2138-2147, Sept. 2009, doi: 10.1109/TPEL.2009.2021762.